ACS APPLIED MATERIALS & INTERFACES

Research Article

www.acsami.org

Robust Thick Polymer Brushes Grafted from Gold Surfaces Using Bidentate Thiol-Based Atom-Transfer Radical Polymerization Initiators

Chul Soon Park, Han Ju Lee, Andrew C. Jamison, and T. Randall Lee*

Department of Chemistry and the Texas Center for Superconductivity, University of Houston, 4800 Calhoun Road, Houston, Texas 77204-5003, United States

Supporting Information

ABSTRACT: A new bromoisobutyrate-terminated alkanethiol, 16-(3,5-bis(mercaptomethyl)phenoxy)hexadecyl 2-bromo-2-methylpropanoate (BMTBM), was designed as a bidentate adsorbate to form thermally stable bromoisobutyrate-terminated self-assembled monolayers (SAMs) on flat gold surfaces to conduct atom-transfer radical polymerizations (ATRPs). The monolayers derived from BMTBM were characterized by ellipsometry, X-ray photoelectron spectroscopy (XPS), and polarization modulation infrared reflection–absorption spectroscopy (PM-IRRAS) and compared to the monolayers formed from 16-mercaptohexadecyl 2-bromo-2-methylpropanoate (MBM), 16-(3-(mercaptomethyl)phenoxy)hexadecyl 2-bromo-2-methyl-propanoate (MTBM), and octadecanethiol (C18SH). In this study, although the monolayer derived from BMTBM was less densely packed than those derived from MBM and MTBM, the bidentate adsorbates demonstrated much higher thermal stability in solution-phase thermal desorption tests, owing to the "chelate effect". The enhanced stability of the BMTBM SAMs ensured the development of thick brushes of poly(methyl methacrylate) and polystyrene at elevated temperatures (60, 90, 105, and 120 °C). In contrast, SAMs derived from MBM and MTBM failed to grow polymer brushes at temperatures above 100 °C.

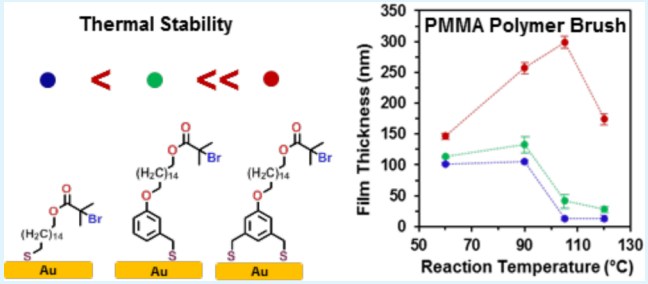

KEYWORDS: *ATRP, SAMs, thermal stability, chelate effect, polymer brushes, PMMA, PS*

INTRODUCTION

The growth of polymer brushes from a plethora of substrates (e.g., nanoparticles, metals, and oxides) has drawn wide interest from researchers as a result of the abundant number of applications for this technology, including their use as anticorrosion coatings, etch masks, lithographic coatings, antifouling coatings, anti-icing treatments, and photocatalytic surfaces.[1−9] To modify the substrates, controlled radical polymerization (CRP) procedures have been developed in chemistry and polymer science, with three CRP systems being the most widely used: stable free-radical polymerization (SFRP),[10] catalytic atom-transfer radical polymerization (ATRP),[11−13] and degenerative chain-transfer polymerization.[14] ATRP is a particularly fascinating method because of the broad range of monomers and solvents available and the relatively simple experimental setup, which enables precise control and versatility in the polymerization procedure.

For ATRP, anchoring the initiator to the substrate is a necessary and crucial first step for successful film formation. Thiols on Au and organosilane compounds on oxide surfaces are the predominate systems that have been pursued because these systems produce well-defined interfaces. With regard to fundamental studies of this surface polymerization process, many researchers have used gold substrates to grow polymer brushes with ATRP because the resultant surfaces are reliably homogeneous and easily analyzed by various techniques, such as X-ray photoelectron spectroscopy (XPS) and polarization modulation infrared reflection–absorption spectroscopy (PM-IRRAS). Thiol-based radical initiators deposited on gold typically form self-assembled monolayers (SAMs) that provide closely packed and well-ordered organic thin films under ambient conditions. ATRP can occur from SAMs that are terminated with radical initiator groups; however, performing ATRP from thiolate SAMs on Au is challenging because the bond between Au and the sulfur atom of the initiator molecules is labile at high temperatures. A potential solution to this problem was originally surmised by Schlenoff et al., who noted in 1995 that the stability of SAMs might be improved by increasing the number of bonds for each adsorbate, a hypothesis that has since been tested and proven correct with a variety of adsorbate structures.[15] Lee et al. recently demonstrated that the desorption of thiols can be significantly decreased by introducing two methylthiol groups attached *meta* to one another on an aromatic ring as bidentate headgroups,

Received: November 22, 2015
Accepted: February 3, 2016
Published: February 3, 2016

DOI: 10.1021/acsami.5b11305
ACS Appl. Mater. Interfaces 2016, 8, 5586−5594

using the chelate effect.[16] Alternatively, Saha et al. investigated the formation of thick brushes of poly(methyl methacrylate) (PMMA) and polystyrene (PS) at high temperatures from ATRP initiators anchored via the cross-linking of (3-mercaptopropyl)trimethoxysilane moieties on gold surfaces.[17]

In this report, we designed, synthesized, and examined the performance of the following three new ATRP initiators in the growth of PMMA and PS brushes from the surface of gold: 16-mercaptohexadecyl 2-bromo-2-methylpropanoate (MBM), 16-(3-(mercaptomethyl)phenoxy)hexadecyl 2-bromo-2-methylpropanoate (MTBM), and 16-(3,5-bis(mercaptomethyl)-phenoxy)hexadecyl 2-bromo-2-methylpropanoate (BMTBM). In particular, the initiator BMTBM was devised to provide enhanced thermal stability through its architecture of having an aromatic ring with two thiol headgroups that can chelate readily to the surface of gold. Figure 1 shows the structures of these new ATRP initiators.

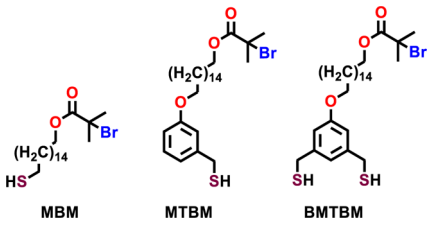

Figure 1. Structures of the adsorbates MBM, MTBM, and BMTBM used for initiating ATRP.

SAMs were prepared on flat gold substrates from MBM, MTBM, and BMTBM, as illustrated in Scheme 1. Additionally, a SAM formed from octadecanethiol (C18SH) was used as a reference system for comparison. All SAMs were characterized using ellipsometry, XPS, and PM-IRRAS. Each of the radical initiator SAMs was subjected to ATRP for 1 h in the presence of either methyl methacrylate or styrene to form films of PMMA or PS, respectively. To evaluate the relative thermal stability of the SAMs derived from the radical initiator adsorbates, we performed solution-phase desorption tests to measure the fraction of each SAM remaining after exposure of the films to 60, 90, 105, and 120 °C in dimethylformamide (DMF)/anisole (1:1, v/v) as a function of time.

EXPERIMENTAL SECTION

Materials. ω-Hexadecalactone, hydrobromic acid (48 wt %), 3,4-dihydropyran, lithium aluminum hydride ($LiAlH_4$), potassium carbonate (K_2CO_3), methanesulfonyl chloride (MsCl), triethylamine (Et_3N), potassium thioacetate (KSAc), dimethyl 5-hydroxyisophthalate, 4-(hydroxymethyl)phenol, and C18SH were purchased from Sigma-Aldrich. Copper(I) bromide (CuBr), copper(II) bromide ($CuBr_2$), and 1,4,8,11-tetramethyl-1,4,8,11-tetraazacyclotetradecane (Me_4Cyclam) were obtained from Sigma-Aldrich. 4,4′-Dinonyl-2,2′-bipyridyl (dnNbpy) was purchased from TCI. The solvents and reagents acetic acid (AcOH), tetrahydrofuran (THF), dichloromethane (CH_2Cl_2), acetonitrile (CH_3CN), methanol (MeOH), chloroform ($CHCl_3$), and methyl methacrylate, were acquired from Sigma-Aldrich. Additionally, hexanes, ethyl acetate (EtOAc), and acetone were purchased from Mallinckrodt Chemicals. The anhydrous ethanol (EtOH) used to develop the SAMs came from Decon Laboratories, Inc. THF and CH_2Cl_2 were dried by distilling over calcium hydride before use. Water was purified to a resistivity of 18 MΩ cm using an Academic Milli-Q Water System (Millipore Corporation) and filtered through a 0.22 μm membrane filter before use. Silica gel for column chromatography was obtained from Sorbent Technologies. Gold pellets (99.999%) were purchased from Kamis, Inc.; chromium-coated rods were acquired from Kurt J. Lesker Co.; and polished silicon (100) wafers were obtained from University Wafer.

Synthesis of the Initiators. The synthetic procedures used to prepare the radical initiator adsorbates (MBM, MTBM, and BMTBM) and their ^{1}H and ^{13}C NMR spectra (Figures S1–S6) are provided in the Supporting Information.

Preparation of Substrates. Flat gold substrates were prepared by the thermal evaporation of gold (~1000 Å) onto chromium-coated (~100 Å) Si wafers under ultrahigh vacuum. The gold-coated wafers were cut into slides (1 × 4 cm), rinsed with ethanol, and dried with ultrapure nitrogen gas. Immediately before insertion in the development solutions, optical constants were collected from three different regions on each slide.

Preparation of SAMs with MBM, MTBM, and BMTBM. The SAMs of each adsorbate were prepared in 1 mM ethanolic solutions in vials cleaned with piranha solution beforehand (3:1 mixture of concentrated H_2SO_4/30 wt % H_2O_2), followed by rinsing with deionized water and ethanol (Caution: piranha solution is highly corrosive, reacts intensely with organic materials, and should be handled with extreme caution). Additionally, we prepared SAMs from C18SH for use as a baseline reference because these SAMs are well-defined and can be used to assist in SAM characterization. All slides were incubated in their ethanolic adsorbate solutions for at least 48 h, followed by washing with THF and ethanol and drying with ultrapure nitrogen gas before characterization.[18]

Growth of Polymer Brushes by Surface-Initiated ATRP. In the glovebox, CuBr (0.040 mmol), $CuBr_2$ (0.040 mmol), Me_4Cyclam (0.040 mmol), and dnNbpy (0.040 mmol) were weighed and introduced into vials that contained 20 mL of a degassed solution comprised of 10 mL of monomer (styrene or methyl methacrylate) and 10 mL of a 50:50 mixture of DMF/anisole by volume, followed by agitation and the introduction of the initiator-coated gold slides prepared as described above. After preparation and capping in the glovebox, the vials were transferred to a preheated oil bath outside of the glovebox and heated at either 60, 90, 105, or 120 °C. After 1 h, the vials were removed from the oil bath, and the gold slides were removed from the vials. The gold slides were washed with THF, ethyl acetate, and ultrapure EtOH before characterization.

Scheme 1. Surface-Initiated Polymerization of PMMA and PS on the Surface of Gold Initiated by SAMs Derived from MBM, MTBM, and BMTBM

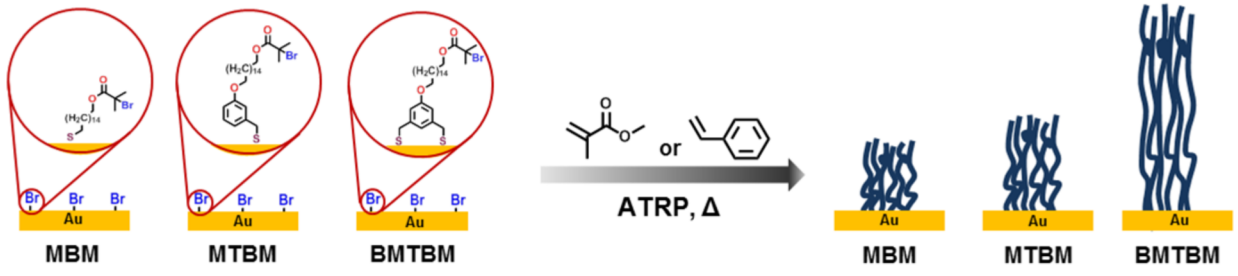

DOI: 10.1021/acsami.5b11305
ACS Appl. Mater. Interfaces 2016, 8, 5586–5594

Thermal Stability Tests. The thermal stability of the radical initiator monolayers and the associated polymer films were determined using a previously established analytical method.[16] The fraction of the SAMs remaining on the gold surfaces was calculated using the ellipsometric thicknesses of the films, before and after heating. Monolayer films generated from initiator molecules were heated in unstirred solutions containing a mixture of DMF/anisole (1:1, v/v) at defined temperatures (60, 90, 105, and 120 °C). Before each thickness measurement, the films were washed with THF and then ethanol and dried with ultrapure nitrogen gas.

Instrumental Procedures for Characterizing the SAMs. The instrumental procedures used to characterize the SAMs formed from MBM, MTBM, and BMTBM are provided in the Supporting Information.

RESULTS AND DISCUSSION

Characterization of SAMs Formed from MBM, MTBM, and BMTBM Radical Initiators. *Ellipsometric Film Thicknesses.* Table 1 shows the ellipsometric thicknesses of the SAMs formed from C18SH, MBM, MTBM, and BMTBM. Within experimental uncertainty (±2 Å), the ellipsometric thicknesses obtained in this study for the SAMs formed from C18SH and MBM correspond well with values for the same or analogous SAM systems found in the literature, indicating that our gold substrates are suitable for forming well-packed SAMs.[16,18] The increase in thickness for the MTBM SAM as compared to the SAM formed from MBM can be rationalized by the insertion of the aromatic ring in the adsorbate structure. However, although the monothiol MTBM and dithiol BMTBM are similar from the perspective of their molecular composition and possess the same adsorbate length from one thiol moiety to the bromide group, the thickness of the film formed from BMTBM is less than that from MTBM. This difference can be rationalized by the fact that the two sulfur headgroups of BMTBM occupy more space on the surface of gold than the single sulfur headgroup of the monodentate adsorbates. As a consequence, the distance between the chains of the chemisorbed BMTBM molecules on the gold surface should be greater, which means that the aliphatic chains of BMTBM must tilt more on the surface to optimize van der Waals interactions between chains.

Table 1. Thicknesses of SAMs Prepared from C18SH, MBM, MTBM, and BMTBM

adsorbate	ellipsometric thickness (Å)[a]	reference thickness (Å)
C18SH	23	22[18]
MBM	23	23[19]
MTBM	29	
BMTBM	24	

[a]Ellipsometric thicknesses were reproducible within ±2 Å.

Analysis of the X-ray Photoelectron Spectra. Spectra collected using XPS provide three crucial types of information regarding SAMs: (1) the binding energy (BE) of the S 2p orbitals can be used to determine the nature and degree of bonding between the sulfur moieties and the gold surface; (2) the positions of the spectral peaks can be used to determine the atomic composition of the SAMs; and (3) certain characteristic BE peaks can be used to calculate the relative packing density of the SAMs compared to a well-defined reference film. Figure 2 provides the X-ray photoelectron spectra for the regions of interest for this particular investigation, verifying the presence of each of the key detectable elements found in our adsorbate structures. For our SAMs, which were prepared on gold surfaces, the Au $4f_{7/2}$ peak at 84.0 eV was used as a reference peak for the BE scales (data not shown). Figure 2A confirms that oxygen was a component of the structures of each of the three initiator monolayers but not of the normal alkanethiolate reference film.

For bound thiolate, the S 2p binding energy peaks appear as a doublet, with the S $2p_{1/2}$ peak located at ~163.2 eV and the S $2p_{3/2}$ peak located at ~162 eV. For unbound thiol/disulfide and oxidized sulfur species, the more intense peak of the doublet, the S $2p_{3/2}$ BE peak, appears at ~163.5−164 and >166 eV, respectively, making it possible to determine if the adsorbates in a thiolate monolayer film are fully bound by carefully examining this region of the spectra.[20]

Figure 2B shows that all adsorbates were well-bound on the gold surfaces, with only minimal levels of unbound sulfur present as well as no oxidized sulfur species. The degree of surface binding was determined by peak fitting the S 2p peaks in the X-ray photoelectron spectra using Multipak software, as shown in Figure S7 and Table S1 of the Supporting Information. Using this approach, the calculated levels of bound thiolate were found to be 99, 94, 92, and 85% for C18SH, MBM, MTBM, and BMTBM, respectively. In Figure 2C, all of the radical initiator films show three different C 1s peaks at ~285, 286, and 289 eV, corresponding to alkyl chain hydrocarbons, C−O−C, and C═O.[16,21] Figure 2D shows the Br 3d peaks for the radical initiator films, revealing peaks at ~70 and 71.6 eV that correspond to Br $3d_{5/2}$ and Br $3d_{3/2}$, respectively.[22] The XPS data confirm that all of the radical

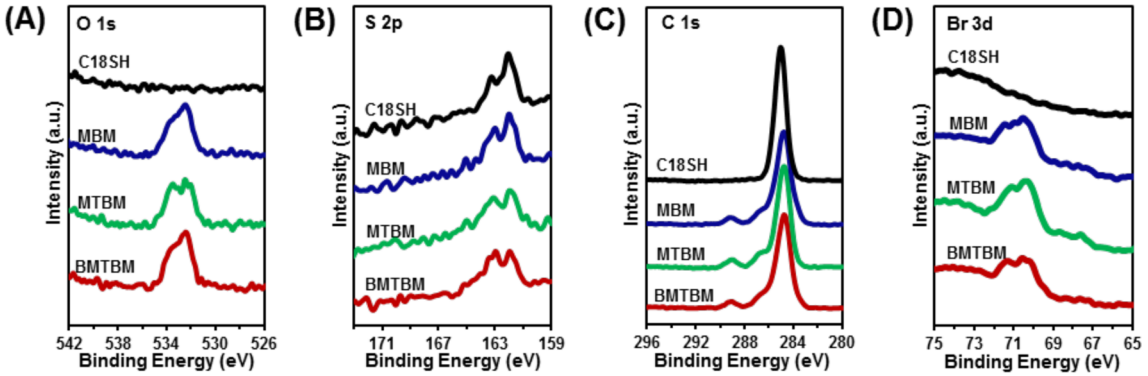

Figure 2. X-ray photoelectron spectra of the (A) O 1s, (B) S 2p, (C) C 1s, and (D) Br 3d spectral regions of the films derived from C18SH, MBM, MTBM, and BMTBM.

DOI: 10.1021/acsami.5b11305
ACS Appl. Mater. Interfaces 2016, 8, 5586−5594

initiator adsorbates form well-bound thin films with similar compositional and structural characteristics. Finally, several previous studies have verified the sensitivity of the C 1s binding energy peak position within the framework of the relative coverage of adsorbates on the substrates.[18,23,24] The C 1s BE peak positions for the methylene carbons are at ~285.0, ~284.8, ~284.7, and ~284.6 eV for C18SH, MBM, MTBM, and BMTBM, respectively, revealing the influence of the terminal group on chain packing (and the headgroup for BMTBM). The BEs of these carbons and the carbons of the aromatic ring for the BMTBM SAMs shift to slightly lower binding energies compared to the other aromatic adsorbate (~0.1 eV). A lower C 1s BE for similarly structured hydrocarbon adsorbates has generally been interpreted as an indication that a positive charge can be more easily discharged because the alkyl chains of the SAMs are less densely packed, which reduces their effectiveness as an insulator. SAMs derived from BMTBM appear to be consistent with this model.[25,26] In further analysis, the integrated areas under the peaks of the bands associated with the S 2p and Au 4f BEs are frequently used to derive sulfur/gold (S/Au) ratios to help characterize the films, as described previously.[16] Using these ratios, we compared the relative packing densities of monolayers derived from the different adsorbates. In this study, the monolayer derived from C18SH is used as a reference film and assumed to represent 100%; furthermore, our analysis assumes that the films have similar thicknesses and that the adsorbates in these films are homogeneously distributed. Using this approach, we determined that the relative packing densities of the adsorbates and, therefore, also the surface density of the initiator-terminated alkyl chains for the SAMs derived from MBM, MTBM, and BMTBM were 86, 75, and 43%, respectively, as compared to SAMs derived from C18SH at 100% (see Table 2). These results are consistent with the X-ray photoelectron spectra in Figure 2B.

Table 2. Relative Packing Densities of the SAMs Derived from the Indicated Adsorbates

	XPS peak area			
adsorbate	Au 4f	S 2p	S/Au	relative packing density (%)
C18SH	93.7	6.3	0.067	100
MBM	94.5	5.5	0.058	86
MTBM	95.2	4.8	0.050	75
BMTBM	94.6	5.4	0.028[a]	43

[a]To compare to the monodentate adsorbates, the S/Au ratio for BMTBM was divided by a factor of 2.

Analysis of the PM-IRRAS Spectra. Surface infrared spectroscopy is a useful tool to determine the general alkyl chain conformational order and to identify characteristic peaks of functional groups for organic thin films. The degree of order for a *n*-alkanethiolate monolayer film and any similarly structured films that rely upon van der Waals attractions between alkyl chains to stabilize the assembly can be evaluated by the band position of the antisymmetric methylene C−H stretching vibration ($\nu_a^{CH_2}$) obtained from PM-IRRAS.[16,27] This analysis is facilitated because a well-packed, highly ordered alkyl chain assembly allows for the chains to organize in their lowest energy conformations, an all *trans*-extended alignment of the carbons. For example, the $\nu_a^{CH_2}$ of a well-ordered heptadecanethiolate SAM appears at ~2919 cm^{-1}, whereas a loosely packed, disordered film derived by a thermal desorption experiment exhibits a $\nu_a^{CH_2}$ at ~2924 cm^{-1}.[28] Figure 3A shows the band positions of $\nu_a^{CH_2}$ for monolayers generated from the adsorbates used in this study: C18SH, MBM, MTBM, and BMTBM produced $\nu_a^{CH_2}$ peaks at 2918, 2920, 2922, and 2924 cm^{-1}, respectively. According to these results, the conformational order or relative "crystalinity" of the monolayer films is as follows: C18SH > MBM > MTBM > BMTBM. These results are consistent with the packing densities inferred from the XPS data (*vida supra*).

As shown in Figure 3B, PM-IRRAS also provides information regarding the characteristic functional groups of the organic thin films formed from MBM, MTBM, and BMTBM. Unlike the C18SH SAM, these SAMs have characteristic peaks for C═O stretching at ~1725 cm^{-1} and C−O stretching at ~1270 cm^{-1}, with both functional groups being present in the tailgroup.[29] Because the C18SH and MBM SAMs contain no aromatic rings, unlike the SAMs formed from MTBM and BMTBM, the infrared (IR) spectra for the former SAMs show no aromatic C═C stretching at ~1600 cm^{-1}, which is present in the spectra for the latter SAMs.[30]

Thermal Stability of the Radical Initiator SAMs on Flat Gold. For ATRP, the polymer growth rate depends upon the monomer, solvent system, and reaction temperature. Generally, this dependence has included a strong correlation between the growth rate of polymerization by ATRP and an increase in the reaction temperature.[31] Indeed, the stability (i.e., stable bonding to the substrate) of the initiator monolayers plays a key role in the growth of polymer brushes on gold surfaces for the MBM, MTBM, and BMTBM SAMs (*vide infra*). A study by Lee et al. that analyzed a series of similarly structured adsorbates revealed that a monodentate thiolate film is unstable at elevated temperatures (>90 °C), while a bidentate thiolate SAM proved to be thermally stable, owing to the "chelate

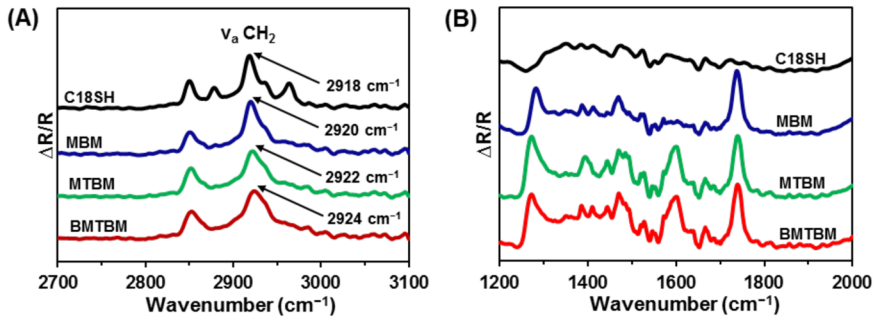

Figure 3. PM-IRRAS spectra of the (A) C−H stretching region and (B) region extending from 1200 to 2000 cm^{-1} for the films formed from C18SH, MBM, MTBM, and BMTBM.

DOI: 10.1021/acsami.5b11305
ACS Appl. Mater. Interfaces 2016, 8, 5586−5594

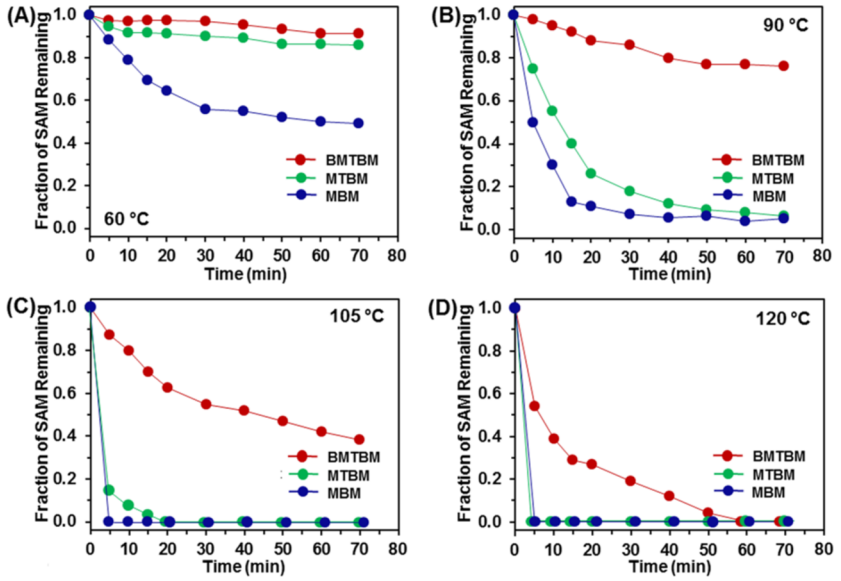

Figure 4. Thermal stability based on solution-phase thermal desorption as determined by ellipsometric thickness measurements for SAMs formed from MBM, MTBM, and BMTBM for heating baths set at (A) 60 °C, (B) 90 °C, (C) 105 °C, and (D) 120 °C in anisole/DMF = 1:1.

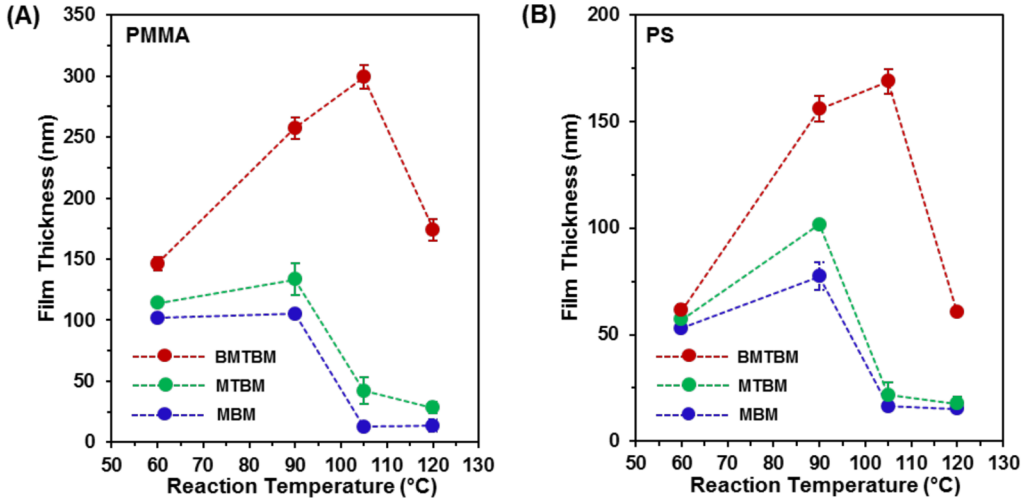

Figure 5. Film thicknesses of polymer brushes grown at elevated temperatures from MBM, MTBM, and BMTBM SAMs as a function of the reaction temperature: (A) PMMA films grown at 60, 90, 105, and 120 °C and (B) PS films grown at 60, 90, 105, and 120 °C. All data were recorded after 1 h of growth. Plots A and B have different *y*-axis scales to provide comparison for the trends between the two types of polymerization processes. Dashed lines connecting data points are included as guides for the eye.

effect".[16] We therefore performed solution-phase thermal desorption studies to evaluate the thermal stability for all monolayers investigated in this report using an established method.[16] For these tests, we immersed the SAMs in a blend of anisole/DMF (1:1, v/v), the same solvents used for polymerization of the PMMA and PS brushes, and then measured the ellipsometric thicknesses at various time intervals using several heating bath temperatures (60, 90, 105, and 120 °C). As shown in Figure 4A, the fraction of the MTBM and BMTBM SAMs remaining after 1 h at 60 °C was over 80%, while for the MBM SAM, the fraction was ∼50%. The enhanced stability of the MTBM SAM plausibly derives from the presence of the aromatic ring, as noted above. However, there is a significant difference in the data in Figure 4B, where only the BMTBM SAM showed strong resistance to desorption, with ∼75% surviving 1 h at 90 °C, with the monolayers derived from MBM and MTBM exhibiting residual film thicknesses below 20% at 90 °C. These results are consistent with previous reports.[16,32] At 105 °C, the fraction of the BMTBM SAM remaining was over 40% after 1 h, and at 120 °C, the fraction of the BMTBM SAM remaining was only 20% after 30 min (plots C and D of Figure 4).

The results of the thermal stability test indicate that the monolayer generated from BMTBM is remarkably stable compared to the monolayers derived from MBM and MTBM at elevated temperatures, an outcome that can be rationalized with the chelate effect.[16,32] On the basis of these results, we can anticipate that the polymer brushes grown from SAMs derived from BMTBM will be thicker than those from MBM and MTBM under the same reaction conditions (e.g., temperature, concentration of monomer, and reaction time). Further, these thermal stability results indicate that the thicknesses of the PMMA and PS brushes grown from the BMTBM SAMs will plausibly reach a maximum at a certain temperature and then

DOI: 10.1021/acsami.5b11305
ACS Appl. Mater. Interfaces 2016, 8, 5586−5594

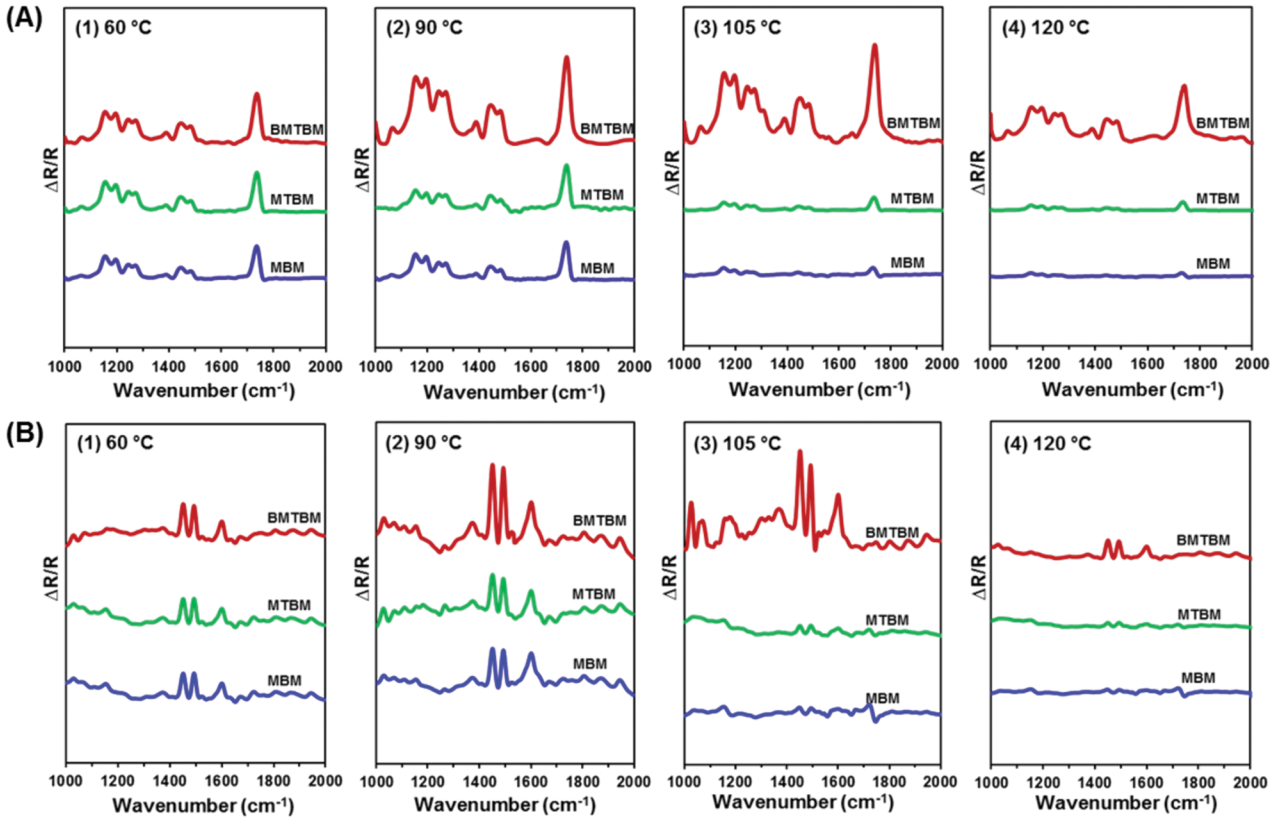

Figure 6. PM-IRRAS spectra of the polymer brush films for the spectral region from 1000 to 2000 cm^{-1} for (A) PMMA films grown at (1) 60 °C, (2) 90 °C, (3) 105 °C, and (4) 120 °C and (B) PS films grown at (1) 60 °C, (2) 90 °C, (3) 105 °C, and (4) 120 °C. All spectra were recorded after 1 h of film growth.

decline with an increasing temperature as the initiator desorbs from the surface.

Thicknesses of the PMMA and PS Polymer Brushes Formed at Elevated Temperatures on Flat Gold. To compare the thicknesses of the polymer brushes that develop in the context of the thermal stability of the SAM, we performed ATRP using the thermal stability test conditions for the SAMs derived from MBM, MTBM, and BMTBM. Figure 5A shows the thickness of the PMMA brushes formed at 60, 90, 105, and 120 °C after 1 h of polymer growth. At 60 °C, the thickness of the PMMA film was similar for all initiators, except for BMTBM, where the film thickness was ∼30 nm more than the films generated from MBM and MTBM. However, the thickness of the resulting PMMA brushes was amplified when the polymerization was performed at 90 °C. At 90 °C, the thickness of the PMMA film is ∼130 nm more for the BMTBM SAMs than the MBM and MTBM SAMs. This difference is also readily apparent in the data for the films formed at 105 and 120 °C; more specifically, the thickness of the PMMA brush derived from BMTBM was ∼300 nm after only 1 h of growth at 105 °C, which was remarkably greater than the brushes generated from the MBM and MTBM radical initiator SAMs. These results can be rationalized by the enhanced thermal stability of the chelating BMTBM adsorbate because surface-initiated ATRP can be quenched by adsorbate radicals that have undergone desorption.[17]

As shown in plots C and D of Figure 4, the adsorbate SAMs derived from MBM and MTBM were totally desorbed after 5 min, while about 50 and 15% of the SAM generated from BMTBM still remained after 40 min at 105 and 120 °C, respectively. Consequently, for MBM and MTBM, there was little or no radical initiator remaining on the surface during most of the experiment. Correspondingly, the residual PMMA thickness on SAMs derived from MBM and MTBM was ∼20 nm at 1 h for the experiments conducted at 120 °C, while that for SAMs derived from BMTBM was ∼170 nm, reflecting the contribution of film integrity that comes from the initiating monolayer. On the basis of these results, we can confirm that the polymerization on the monolayers with thiol-based adsorbates highly depends upon the thermal stability of the initiating monolayers. Moreover, the growth rate of the polymer brushes varies with the reaction temperature in a predictable manner, as illustrated by the increasing PMMA film thicknesses for the polymer brushes grown from the BMTBM monolayers (up to 105 °C), despite the desorption of adsorbate molecules that was revealed in Figure 4. However, the thicknesses of the BMTBM-derived polymer films exhibit a remarkable reduction at 120 °C because even this bidentate adsorbate desorbs at 120 °C.

For PS polymer brushes, the trends are exactly the same as the PMMA brushes, with the only difference being that the thicknesses of PS films are less than those of the PMMA films under the same reaction conditions. As was expected, the PMMA films formed from all of the radical initiator adsorbates examined in this study had thickness maxima that reflected the stability of the individual adsorbate; for BMTBM, these maxima occurred at a higher temperature, 105 °C. According to these results, we can conclude that the thermal stability of the adsorbates (MBM, MTBM, and BMTBM) have a remarkable influence on the growth of polymer brushes grown from gold

DOI: 10.1021/acsami.5b11305
ACS Appl. Mater. Interfaces 2016, 8, 5586−5594

surfaces. As shown in Table 2, the relative packing density of the SAMs derived with BMTBM is much lower than that of the SAMs formed from MBM and MTBM. Notably, the thickness of a particular type of polymer brush has been shown to increase with initiator density.[19] Correspondingly, the thickness of a polymer brush derived from BMTBM would be expected to be lower because the relative surface density of the reactive sites for the SAMs formed from BMTBM is much lower than that of the other initiators. However, the thicknesses of the polymer brushes grown with BMTBM are much higher under all reaction conditions, which we attribute to the marked differences in thermal stability of the initiator monolayers (see Figure 4).

To provide a more detailed comparison of the polymer brushes developed in this study, we collected PM-IRRAS spectra for the films grown under the different reaction temperatures. Using the PM-IRRAS data, we conducted a qualitative comparison of the polymer chains that form the brushes based on the intensity of characteristic peaks and verified that the films detected by ellipsometry are indeed the targeted polymer films. Figure 6 shows the results that were obtained for the PMMA and PS brushes described in the text above with regard to Figure 5. The PMMA brushes exhibit a sharp band at 1734 cm^{-1} corresponding to the C═O stretch,[33,34] and an analysis of the PM-IRRAS spectra of the PS homopolymer brushes reveal characteristic peaks for the aromatic C═C stretching vibrations at 1447 and 1490 cm^{-1}.[35,36] As shown in Figure 6, the PM-IRRAS spectra of both the PMMA and PS polymer brushes are in excellent agreement with the reported reference IR spectra. Additionally, in plot 1 of Figure 6A, the intensity of the C═O band of the PMMA brushes is similar for each of the polymer films, which can be rationalized by the similar thermal stability of all of these films at 60 °C. However, the film developed from the monolayer derived from BMTBM (the bidentate adsorbate) exhibits a much higher intensity for the C═O stretching vibration than the films generated from MBM and MTBM at 90 °C after 1 h (plot 2 of Figure 6A). At 105 °C, the intensity of the peaks for the films derived from MBM and MTBM were significantly lower than that for the film formed from BMTBM (plot 3 of Figure 6A). Furthermore, at 120 °C, all three PMMA films show significant decreases in peak intensities (see plot 4 of Figure 6A). These results are consistent with the film thicknesses shown in Figure 5A. According to the spectra in Figure 6B, the PS films also exhibit trends for their intensities that align with the results found in Figure 5B, using the peaks at 1447 and 1490 cm^{-1} as the characteristic peaks for these films. According to these results, we can confirm that the growth of the polymer brushes is highly related to the thermal stability of the preformed radical initiator monolayer.

To confirm the maximum thickness of the PMMA films that can be achieved with our bidentate adsorbate, we also carried out polymerizations at 100 and 110 °C, with the compiled results presented in Figure 7. The thicknesses of the PMMA films produced from the radical initiator BMTBM monolayer exhibit a maxima at 105 °C, indicating this temperature to be optimal for the growth of polymer brushes.

CONCLUSION

A series of thiol-based adsorbates, MBM, MTBM, and BMTBM, was successfully synthesized and used to prepare radical initiator monolayers for the purpose of growing PMMA and PS polymer brushes on the surface of gold. The SAMs prepared from these adsorbates were shown by ellipsometry to have thicknesses that were in line with similar films found in the literature. PM-IRRAS and XPS were used to help characterize the SAMs, providing evidence of the presence of the anticipated elemental components, the key functional groups, and other commonly observed structural features for such SAMs and producing an overall impression that each of the films was generally well-ordered. The newly designed bidentate ATRP initiator, BMTBM, was shown to generate a well-packed monolayer film with over 85% of the sulfur atoms attached to the surface of gold. Although the packing density and conformational order of the monolayer derived from BMTBM was less than the monolayers derived from the monodentate adsorbates MBM and MTBM, the thermal stability of the BMTBM SAM proved to be much higher. The enhanced stability was attributed to the formation of multiple bonds between the adsorbate and the surface of gold via the "chelate effect". The thermal stability of the monolayer formed from BMTBM was shown to facilitate the growth of thick polymer brushes within 1 h at higher reaction temperatures than can be accessed using monodentate adsorbates. Further, according to our results, the successful growth of polymer brushes, such as PMMA and PS, highly depends upon the thermal stability of the underlying radical initiator monolayer. Additionally, the thicknesses of these polymer films were maximized with the use of the BMTBM adsorbate at 105 °C, owing to its superior thermal stability when bound to gold.

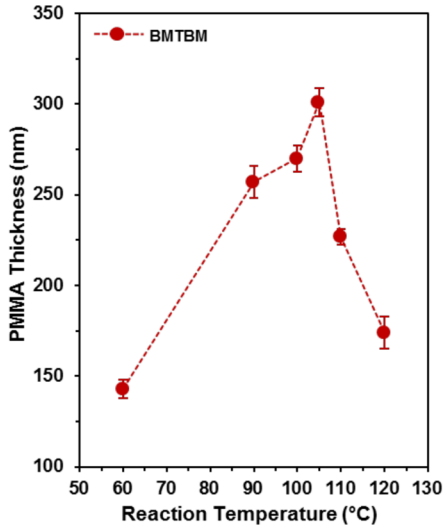

Figure 7. Thickness profiles for the PMMA brushes grown on radical initiator monolayers derived from BMTBM at 60, 90, 100, 105, 110, and 120 °C after 1 h of film growth.

ASSOCIATED CONTENT

Supporting Information

The Supporting Information is available free of charge on the ACS Publications website at DOI: 10.1021/acsami.5b11305.

Detailed descriptions of the synthetic procedures for bromoisobutyrate-terminated thiols (MBM, MTBM, and BMTBM) along with the ^{1}H and ^{13}C NMR spectra of MBM, MTBM, and BMTBM (PDF)

DOI: 10.1021/acsami.5b11305
ACS Appl. Mater. Interfaces 2016, 8, 5586−5594

AUTHOR INFORMATION

Corresponding Author

*E-mail: trlee@uh.edu.

Notes

The authors declare no competing financial interest.

ACKNOWLEDGMENTS

The authors thank the National Science Foundation (CHE-1411265), the Robert A. Welch Foundation (Grant E-1320), and the Texas Center for Superconductivity at the University of Houston for generous support.

REFERENCES

(1) Lu, G.; Li, Y.-M.; Lu, C.-H.; Xu, Z.-Z. Corrosion Protection of Iron Surface Modified by Poly(methyl methacrylate) Using Surface-Initiated Atom Transfer Radical Polymerization (SI-ATRP). *Colloid Polym. Sci.* **2010**, *288*, 1445−1455.

(2) García, T. A.; Gervasi, C. A.; Rodríguez Presa, M. J.; Otamendi, J. I.; Moya, S. E.; Azzaroni, O. Molecular Transport in Thin Thermoresponsive Poly(*N*-isopropylacrylamide) Brushes with Varying Grafting Density. *J. Phys. Chem. C* **2012**, *116*, 13944−13953.

(3) Li, M.; Neoh, K. G.; Xu, L. Q.; Wang, R.; Kang, E.-T.; Lau, L.; Olszyna, D. P.; Chiong, E. Surface Modification of Silicone for Biomedical Applications Requiring Long-Term Antibacterial, Antifouling, and Hemocompatible Properties. *Langmuir* **2012**, *28*, 16408−16422.

(4) Zhao, C.; Zheng, J. Synthesis and Characterization of Poly(*N*-hydroxyethylacrylamide) for Long-Term Antifouling Ability. *Biomacromolecules* **2011**, *12*, 4071−4079.

(5) Raghuraman, G. K.; Dhamodharan, R.; Prucker, O.; Ruhe, J. A Robust Method for the Immobilization of Polymer Molecules on SiO_2 Surfaces. *Macromolecules* **2008**, *41*, 873−878.

(6) Genua, A.; Alduncín, J. A.; Pomposo, J. A.; Grande, H.; Kehagias, N.; Reboud, V.; Sotomayor, C.; Mondragon, I.; Mecerreyes, D. Functional Patterns Obtained by Nanoimprinting Lithography and Subsequent Growth of Polymer Brushes. *Nanotechnology* **2007**, *18*, 215301.

(7) Chen, H.; Zhang, M.; Yang, J.; Zhao, C.; Hu, R.; Chen, Q.; Chang, Y.; Zheng, J. Synthesis and Characterization of Antifouling Poly(*N*-acryloylaminoethoxyethanol) with Ultralow Protein Adsorption and Cell Attachment. *Langmuir* **2014**, *30*, 10398−10409.

(8) Chernyy, S.; Jarn, M.; Shimizu, K.; Swerin, A.; Pedersen, S. U.; Daasbjerg, K.; Makkonen, L.; Claesson, P.; Iruthayaraj, J. Superhydrophilic Polyelectrolyte Brush Layers with Imparted Anti-Icing Properties: Effect of Counter ions. *ACS Appl. Mater. Interfaces* **2014**, *6*, 6487−6496.

(9) Yoon, M.; Lee, J. -E; Jang, Y. J.; Lim, J. W.; Rani, A.; Kim, D. H. Comprehensive Study on the Controlled Plasmon-Enhanced Photocatalytic Activity of Hybrid Au/ZnO Systems Mediated by Thermoresponsive Polymer Linkers. *ACS Appl. Mater. Interfaces* **2015**, *7*, 21073−21081.

(10) Moreira, G.; Charles, L.; Major, M.; Vacandio, F.; Guillaneuf, Y.; Lefay, C.; Gigmes, D. Stability of SG1 Nitroxide towards Unprotected Sugar and Lithium Salts: a Preamble to Cellulose Modification by Nitroxide-Mediated Graft Polymerization. *Beilstein J. Org. Chem.* **2013**, *9*, 1589−1600.

(11) Wang, J. S.; Matyjaszewski, K. Controlled/"Living" Radical Polymerization. Atom Transfer Radical Polymerization in the Presence of Transition-Metal Complexes. *J. Am. Chem. Soc.* **1995**, *117*, 5614−5615.

(12) Kato, M.; Kamigaito, M.; Sawamoto, M.; Higashimura, T. Polymerization of Methyl Methacrylate with the Carbon Tetrachloridel/Dichlorotris(triphenylphosphine)-ruthedum(II)/Methylaluminum Bis(2,6-di-tert-butylphenoxide) Initiating System: Possibility of Living Radical Polymerization. *Macromolecules* **1995**, *28*, 1721−1723.

(13) Matyjaszewski, K.; Tsarevsky, N. V. Nanostructured Functional Materials Prepared by Atom Transfer Radical Polymerization. *Nat. Chem.* **2009**, *1*, 276−288.

(14) Matyjaszewski, K.; Gaynor, S.; Wang, J. S. Controlled Radical Polymerizations: The Use of Alkyl Iodides in Degenerative Transfer. *Macromolecules* **1995**, *28*, 2093−2095.

(15) Schlenoff, J. B.; Li, M.; Ly, H. Stability and Self-Exchange in Alkanethiol Monolayers. *J. Am. Chem. Soc.* **1995**, *117*, 12528−12536.

(16) Lee, H. J.; Jamison, A. C.; Yuan, Y.; Li, C.-H.; Rittikulsittichai, S.; Rusakova, I.; Lee, T. R. Robust Carboxylic Acid-Terminated Organic Thin Films and Nanoparticle Protectants Generated from Bidentate Alkanethiols. *Langmuir* **2013**, *29*, 10432−10439.

(17) Saha, S.; Bruening, M. L.; Baker, G. L. Facile Synthesis of Thick Films of Poly(methyl methacrylate), Poly(styrene), and Poly(vinyl pyridine) from Au Surfaces. *ACS Appl. Mater. Interfaces* **2011**, *3*, 3042−3048.

(18) Bain, C. D.; Troughton, E. B.; Tao, Y. T.; Evall, J.; Whitesides, G. M.; Nuzzo, R. G. Formation of Monolayer Films by the Spontaneous Assembly of Organic Thiols from Solution onto Gold. *J. Am. Chem. Soc.* **1989**, *111*, 321−340.

(19) Jones, D. M.; Brown, A. A.; Huck, W. T. S. Surface-Initiated Polymerizations in Aqueous Media: Effect of Initiator Density. *Langmuir* **2002**, *18*, 1265−1269.

(20) Castner, D. G.; Hinds, K.; Grainger, D. W. X-ray Photoelectron Spectroscopy Sulfur 2p Study of Organic Thiol and Disulfide Binding Interactions with Gold Surfaces. *Langmuir* **1996**, *12*, 5083−5086.

(21) Lee, B. S.; Chi, Y. S.; Lee, K.-B.; Kim, Y.-G.; Choi, I. S. Functionalization of Poly(oligo(ethylene glycol) methacrylate) Films on Gold and Si/SiO_2 for Immobilization of Protein and Cells: SPR and QCM Studies. *Biomacromolecules* **2007**, *8*, 3922−3929.

(22) de los Santos Pereira, A.; Kostina, N. Y.; Bruns, M.; Rodriguez-Emmenegger, C.; Barner-Kowollik, C. Phototriggered Functionalization of Hierarchically Structured Polymer Brushes. *Langmuir* **2015**, *31*, 5899−5907.

(23) Biebuyck, H. A.; Bain, C. D.; Whitesides, G. M. Comparison of Organic Monolayers on Polycrystalline Gold Spontaneously Assembled from Solutions Containing Dialkyl Disulfides or Alkanethiols. *Langmuir* **1994**, *10*, 1825−1831.

(24) Park, J.-S.; Vo, A. N.; Barriet, D.; Shon, Y.-S.; Lee, T. R. Systematic Control of the Packing Density of Self-assembled Monolayers Using Bidentate and Tridentate Chelating Alkanethiols. *Langmuir* **2005**, *21*, 2902−2911.

(25) Ishida, T.; Nishida, N.; Tsuneda, S.; Hara, M.; Sasabe, H.; Knoll, W. Alkyl Chain Length Effect on Growth Kinetics of *n*-Alkanethiol Self-Assembled Monolayers on Gold Studied by X-Ray Photoelectron Spectroscopy. *Jpn. J. Appl. Phys.* **1996**, *35*, L1710−L1713.

(26) Ishida, T.; Hara, M.; Kojima, I.; Tsuneda, S.; Nishida, N.; Sasabe, H.; Knoll, W. High Resolution X-ray Photoelectron Spectroscopy Measurements of Octadecanethiol Self-Assembled Monolayers on Au(111). *Langmuir* **1998**, *14*, 2092−2096.

(27) Shon, Y.-S.; Lee, S.; Colorado, R.; Perry, S. S.; Lee, T. R. Spiroalkanedithiol-Based SAMs Reveal Unique Insight into the Wettabiities and Frictional Properties of Organic Thin Films. *J. Am. Chem. Soc.* **2000**, *122*, 7556−7563.

(28) Shon, Y.-S.; Lee, T. R. Desorption and Exchange of Self-Assembled Monolayers (SAMs) on Gold Generated from Chelating Alkanedithiols. *J. Phys. Chem. B* **2000**, *104*, 8192−8200.

(29) Retsch, M.; Walther, A.; Loos, K.; Muller, A. H. E. Synthesis of Dense Poly(acrylic acid) Brushes and Their Interaction with Amine-Functional Silsesquioxane Nanoparticles. *Langmuir* **2008**, *24*, 9421−9429.

(30) Faull, J. D.; Gupta, V. K. Selective Guest-Host Association on Self-Assembled Monolayers of Calix[4]resorcinarene. *Langmuir* **2001**, *17*, 1470−1476.

(31) Seeliger, F.; Matyjaszewski, K. Temperature Effect on Activation Rate Constants in ATRP: New Mechanistic Insights into the Activation Process. *Macromolecules* **2009**, *42*, 6050−6055.

(32) Garg, N.; Carrasquillo-Molina, E.; Lee, T. R. Self-Assembled Monolayers Composed of Aromatic Thiols on Gold: Structural

DOI: 10.1021/acsami.5b11305
ACS Appl. Mater. Interfaces 2016, 8, 5586−5594

Characterization and Thermal Stability in Solution. *Langmuir* **2002**, *18*, 2717−2726.
(33) Tretinnikov, O. N.; Ohta, K. Conformation-Sensitive Infrared Bands and Conformational Characteristics of Stereoregular Poly(methyl methacrylate)s by Variable-Temperature FTIR Spectroscopy. *Macromolecules* **2002**, *35*, 7343−7353.
(34) Marutani, E.; Yamamoto, S.; Ninjbadgar, T.; Tsujii, Y.; Fukuda, T.; Takano, M. Surface-Initiated Atom Transfer Radical Polymerization of Methyl Methacrylate on Magnetite Nanoparticles. *Polymer* **2004**, *45*, 2231−2235.
(35) Boyes, S. G.; Brittain, W. J.; Weng, X.; Cheng, S. Z. D. Synthesis, Characterization, and Properties of ABA Type Triblock Copolymer Brushes of Styrene and Methyl Acrylate Prepared by Atom Transfer Radical Polymerization. *Macromolecules* **2002**, *35*, 4960−4967.
(36) Granville, A. M.; Boyes, S. G.; Akgun, B.; Foster, M. D.; Brittain, W. J. Synthesis and Characterization of Stimuli-Responsive Semifluorinated Polymer Brushes Prepared by Atom Transfer Radical Polymerization. *Macromolecules* **2004**, *37*, 2790−2796.

DOI: 10.1021/acsami.5b11305
ACS Appl. Mater. Interfaces 2016, 8, 5586−5594